

# Random Features for Compositional Kernels

Amit Daniely\*   Roy Frostig   Vineet Gupta   Yoram Singer

March 24, 2017

## Abstract

We describe and analyze a simple random feature scheme (RFS) from prescribed compositional kernels. The compositional kernels we use are inspired by the structure of convolutional neural networks and kernels. The resulting scheme yields sparse and efficiently computable features. Each random feature can be represented as an algebraic expression over a *small* number of (random) paths in a composition tree. Thus, compositional random features can be stored compactly. The discrete nature of the generation process enables de-duplication of repeated features, further compacting the representation and increasing the diversity of the embeddings. Our approach complements and can be combined with previous random feature schemes.

arXiv:1703.07872v1 [cs.LG] 22 Mar 2017

---

\*Google Brain, {amitdaniely, frostig, vineet, singer}@google.com

# 1 Introduction

Before the resurgence of deep architectures, kernel methods [22, 21, 18] achieved state of the art results in various supervised learning tasks. Learning using kernel representations amounts to convex optimization with provable convergence guarantees. The first generation of kernel functions in machine learning were oblivious to spatial or temporal characteristics of input spaces such as text, speech, and images. A natural way to capture local spatial or temporal structure is through hierarchical structures using compositions of kernels, see for instance [19, 9]. Compositional kernels became more prominent among kernel methods following the success of deep networks and, for several tasks, they currently achieve the state of the art among all kernel methods [4, 3, 14, 13].

While the “kernel trick” unleashes the power of convex optimization, it comes with a large computational cost as it requires storing or repeatedly computing kernel products between pairs of examples. Rahimi and Recht [16] described and analyzed an elegant and computationally effective way that mitigates this problem by generating random features that approximate certain kernels. Their work was extended to various other kernels [10, 15, 2, 1].

In this paper we describe and analyze a simple random feature generation scheme from prescribed compositional kernels. The compositional kernels we use are inspired by the structure of neural networks. The kernels’ definition and the connection to networks was developed in [6, 5]. Our feature map construction has several benefits over previous ones. It naturally exploits hierarchical structure in terms of representation power. The random feature generation is computationally efficient. More importantly, computing the feature map is efficient and often can be performed in time linear in the embedding dimension. Last but not least, computing the feature map requires highly sparse access patterns to the input, implying low memory requirements in the process.

The course of the paper is as follows. After a brief background, we start the paper by recapping in Sec. 3 the notion of random features schemes (RFS). Informally speaking, a random feature scheme is an embedding from an input space into the real or complex numbers. The scheme is random such that multiple instantiations result in different mappings. Standard inner products in the embedded space emulate a kernel function and converge to the inner product that the kernel defines. We conclude the section with a derivation of concentration bounds for kernel approximation by RFS and a generalization bound for learning with RFS.

The subsequent sections provide the algorithmic core of the paper. In Sec. 4 we describe RFS for basic spaces such as  $\{-1, +1\}$ ,  $[n]$ , and  $\mathbb{T}$ . We show that the standard inner product on the sphere in one and two dimensions admits an effective norm-efficient RFS. However, any RFS for  $\mathbb{S}^{d-1}$  where  $d \geq 3$  is norm-deficient. In Sec. 5, we discuss how to build random feature schemes from compositional kernels that are described by a *computation skeleton*, which is an annotated directed acyclic graph. The base spaces constitute the initial nodes of the skeleton. As the name implies, a compositional kernel consists of a succession of compositions of prior constructed kernels, each of which is by itself a compositional kernel or a base kernel. We conclude the section with run-time and sparsity-level analysis.

The end result of our construction is a lightweight yet flexible feature generation procedure. Each random feature can be represented as an algebraic expression over of a *small* number of (random) paths in a composition tree. Thus, compositional random features

can be stored very compactly. The discrete nature of the generation process enables deduplication of repeated features, further compacting the representation and increasing the diversity of the embeddings. The latter property cannot be directly achieved by previously studied random feature schemes. We would like to emphasize that our approach does not stand in contrast to, but rather complements, prior work. Indeed, the base kernels of a compositional kernel can be non-elementary such as the Gaussian kernel, and hence our RFS can be used in conjunction with the well-studied RFS of [16] for Gaussian kernels. One can also envision a hybrid structure where the base kernels are defined, for example, through a PSD matrix obtained by metric learning on the original input space.

## 2 Background and notation

We start with a few notational conventions used throughout the paper. The Hilbert spaces we consider are over the reals. This includes spaces that are usually treated as complex Hilbert spaces. For example, for  $z = a + ib, z' = a' + ib' \in \mathbb{C}$  we denote  $\langle z, z' \rangle = \text{Re}(z\bar{z}') = aa' + bb'$  (rather than the more standard  $\langle z, z' \rangle = z\bar{z}'$ ). Likewise, for  $\mathbf{z}, \mathbf{z}' \in \mathbb{C}^q$  we denote  $\langle \mathbf{z}, \mathbf{z}' \rangle = \sum_{i=1}^q \langle z_i, z'_i \rangle$ . For a measure space  $(\Omega, \mu)$ ,  $L^2(\Omega)$  denotes the space of square integrable functions  $f : \Omega \rightarrow \mathbb{C}$ . For  $f, g \in L^2(\Omega)$  we denote  $\langle f, g \rangle_{L^2(\Omega)} = \int_{\Omega} \langle f(x), g(x) \rangle d\mu(x)$ . For all the measurable spaces we consider, we assume that singletons are measurable. We denote  $\mathbb{T} = \{z \in \mathbb{C} : |z| = 1\}$ .

Next, we introduce the notation for kernel spaces and recap some of their properties. A *kernel* is a function  $k : \mathcal{X} \times \mathcal{X} \rightarrow \mathbb{R}$  such that for every  $\mathbf{x}_1, \dots, \mathbf{x}_m \in \mathcal{X}$  the matrix  $\{k(\mathbf{x}_i, \mathbf{x}_j)\}_{i,j}$  is positive semi-definite. We say that  $k$  is *D-bounded* if  $k(\mathbf{x}, \mathbf{x}) \leq D^2$  for every  $\mathbf{x} \in \mathcal{X}$ . We call  $k$  a *normalized kernel* if  $k(\mathbf{x}, \mathbf{x}) = 1$  for every  $\mathbf{x} \in \mathcal{X}$ . We will always assume that kernels are normalized. A *kernel space* is a Hilbert space  $\mathcal{H}$  of functions from  $\mathcal{X}$  to  $\mathbb{R}$  such that for every  $\mathbf{x} \in \mathcal{X}$  the linear functional  $f \in \mathcal{H} \mapsto f(\mathbf{x})$  is bounded. The following theorem describes a one-to-one correspondence between kernels and kernel spaces.

**Theorem 1.** *For every kernel  $k$  there exists a unique kernel space  $\mathcal{H}_k$  such that for every  $\mathbf{x}, \mathbf{x}' \in \mathcal{X}$ ,  $k(\mathbf{x}, \mathbf{x}') = \langle k(\cdot, \mathbf{x}), k(\cdot, \mathbf{x}') \rangle_{\mathcal{H}_k}$ . Likewise, for every kernel space  $\mathcal{H}$  there is a kernel  $k$  for which  $\mathcal{H} = \mathcal{H}_k$ .*

The following theorem underscores a tight connection between kernels and embeddings of  $\mathcal{X}$  into Hilbert spaces.

**Theorem 2.** *A function  $k : \mathcal{X} \times \mathcal{X} \rightarrow \mathbb{R}$  is a kernel if and only if there exists a mapping  $\phi : \mathcal{X} \rightarrow \mathcal{H}$  to some Hilbert space for which  $k(\mathbf{x}, \mathbf{x}') = \langle \phi(\mathbf{x}), \phi(\mathbf{x}') \rangle_{\mathcal{H}}$ . In this case,  $\mathcal{H}_k = \{f_{\mathbf{v}} \mid \mathbf{v} \in \mathcal{H}\}$  where  $f_{\mathbf{v}}(\mathbf{x}) = \langle \mathbf{v}, \phi(\mathbf{x}) \rangle_{\mathcal{H}}$ . Furthermore,  $\|f\|_{\mathcal{H}_k} = \min\{\|\mathbf{v}\|_{\mathcal{H}} \mid f = f_{\mathbf{v}}\}$  and the minimizer is unique.*

We say that  $f : [-1, 1] \rightarrow \mathbb{R}$  is a normalized *positive semi-definite* (PSD) function if

$$f(\rho) = \sum_{i=0}^{\infty} a_i \rho^i \text{ where } \sum_{i=0}^{\infty} a_i = 1, \forall i : a_i \geq 0.$$

Note that  $f$  is PSD if and only if  $f \circ k$  is a normalized kernel for any normalized kernel  $k$ .

### 3 Random feature schemes

Let  $\mathcal{X}$  be a measurable space and let  $k : \mathcal{X} \times \mathcal{X} \rightarrow \mathbb{R}$  be a normalized kernel. A *random features scheme* (RFS) for  $k$  is a pair  $(\psi, \mu)$  where  $\mu$  is a probability measure on a measurable space  $\Omega$ , and  $\psi : \Omega \times \mathcal{X} \rightarrow \mathbb{C}$  is a measurable function, such that

$$\forall \mathbf{x}, \mathbf{x}' \in \mathcal{X}, \quad k(\mathbf{x}, \mathbf{x}') = \mathbb{E}_{\omega \sim \mu} \left[ \psi(\omega, \mathbf{x}) \overline{\psi(\omega, \mathbf{x}')} \right].$$

Since the kernel is real valued, we have in this case that,

$$\begin{aligned} k(\mathbf{x}, \mathbf{x}') &= \operatorname{Re}(k(\mathbf{x}, \mathbf{x}')) \\ &= \mathbb{E}_{\omega \sim \mu} \left[ \operatorname{Re} \left( \psi(\omega, \mathbf{x}) \overline{\psi(\omega, \mathbf{x}')} \right) \right] \\ &= \mathbb{E}_{\omega \sim \mu} \langle \psi(\omega, \mathbf{x}), \psi(\omega, \mathbf{x}') \rangle. \end{aligned} \tag{1}$$

We often refer to  $\psi$  as a random feature scheme. We define the *norm* of  $\psi$  as  $\|\psi\| = \sup_{\omega, \mathbf{x}} |\psi(\omega, \mathbf{x})|$ . We say that  $\psi$  is *C-bounded* if  $\|\psi\| \leq C$ . As the kernels are normalized, (1) implies that  $\|\psi\| \geq 1$  always. In light of this, we say that an RFS  $\psi$  is *norm-efficient* if it is 1-bounded. Note that in this case, since the kernel is normalized, it holds that  $|\psi(\omega, \mathbf{x})| = 1$  for almost every  $\omega$  as otherwise we would obtain that  $k(\mathbf{x}, \mathbf{x}) < 1$ . Hence, we can assume w.l.o.g. that the range of norm-efficient RFSs is  $\mathbb{T}$ .

**Comment 1** (From complex to real RFSs). While complex-valued features would simplify the analysis of random feature schemes, it is often favorable to work in practice with real-valued features. Let  $\psi(\omega, \mathbf{x}) := R_\omega(\mathbf{x})e^{i\theta_\omega(\mathbf{x})}$  be a  $C$ -bounded RFS for  $k$ . Consider the RFS

$$\psi'((\omega, b), \mathbf{x}) := \sqrt{2}R_\omega(\mathbf{x}) \cos(\theta_\omega(\mathbf{x}) + b),$$

where  $\omega \sim \mu$ , and  $b \in \{0, \frac{\pi}{2}\}$  is distributed uniformly and independently from  $\omega$ . It is not difficult to verify that  $\psi'$  is  $\sqrt{2}C$ -bounded RFS for  $k$ .

A random *feature* generated from  $\psi$  is a random function  $\psi(\omega, \cdot)$  from  $\mathcal{X}$  to  $\mathbb{C}$  where  $\omega \sim \mu$ . A random *q-embedding* generated from  $\psi$  is the random mapping

$$\Psi_\omega(\mathbf{x}) \stackrel{\text{def}}{=} \frac{(\psi(\omega_1, \mathbf{x}), \dots, \psi(\omega_q, \mathbf{x}))}{\sqrt{q}},$$

where  $\omega_1, \dots, \omega_q \sim \mu$  are i.i.d. The random *q-kernel* corresponding to  $\Psi_\omega$  is  $k_\omega(\mathbf{x}, \mathbf{x}') = \langle \Psi_\omega(\mathbf{x}), \Psi_\omega(\mathbf{x}') \rangle$ . Likewise, the random *q-kernel space* corresponding to  $\Psi_\omega$  is  $\mathcal{H}_{k_\omega}$ . For the rest of this section, let us fix a  $C$ -bounded RFS  $\psi$  for a normalized kernel  $k$  and a random  $q$  embedding  $\Psi_\omega$ . For every  $\mathbf{x}, \mathbf{x}' \in \mathcal{X}$

$$k_\omega(\mathbf{x}, \mathbf{x}') = \frac{1}{q} \sum_{i=1}^q \langle \psi(\omega_i, \mathbf{x}), \psi(\omega_i, \mathbf{x}') \rangle$$

is an average of  $q$  independent random variables whose expectation is  $k(\mathbf{x}, \mathbf{x}')$ . By Hoeffding's bound we have the following theorem.

**Theorem 3** (Kernel Approximation). *Assume that  $q \geq \frac{2C^4 \log(\frac{2}{\delta})}{\epsilon^2}$ , then for every  $\mathbf{x}, \mathbf{x}' \in \mathcal{X}$  we have  $\Pr(|k_\omega(\mathbf{x}, \mathbf{x}') - k(\mathbf{x}, \mathbf{x}')| \geq \epsilon) \leq \delta$ .*

We next discuss approximation of functions in  $\mathcal{H}_k$  by functions in  $\mathcal{H}_{k_\omega}$ . It would be useful to consider the embedding

$$\mathbf{x} \mapsto \Psi^{\mathbf{x}} \text{ where } \Psi^{\mathbf{x}} \stackrel{\text{def}}{=} \psi(\cdot, \mathbf{x}) \in L^2(\Omega). \quad (2)$$

From (1) it holds that for any  $\mathbf{x}, \mathbf{x}' \in \mathcal{X}$ ,  $k(\mathbf{x}, \mathbf{x}') = \langle \Psi^{\mathbf{x}}, \Psi^{\mathbf{x}'} \rangle_{L^2(\Omega)}$ . In particular, from Theorem 2, for every  $f \in \mathcal{H}_k$  there is a unique function  $\check{f} \in L^2(\Omega)$  such that  $\|f\|_{\mathcal{H}_k} = \|\check{f}\|_{L^2(\Omega)}$  and for every  $\mathbf{x} \in \mathcal{X}$ ,

$$f(\mathbf{x}) = \langle \check{f}, \Psi^{\mathbf{x}} \rangle_{L^2(\Omega)} = \mathbb{E}_{\omega \sim \mu} \langle \check{f}(\omega), \psi(\omega, \mathbf{x}) \rangle. \quad (3)$$

Let us denote  $f_\omega(\mathbf{x}) = \frac{1}{q} \sum_{i=1}^q \langle \check{f}(\omega_i), \psi(\omega_i, \mathbf{x}) \rangle$ . From (3) we have that  $\mathbb{E}_\omega [f_\omega(\mathbf{x})] = f(\mathbf{x})$ . Furthermore, for every  $\mathbf{x}$ , the variance of  $f_\omega(\mathbf{x})$  is at most

$$\begin{aligned} \frac{1}{q} \mathbb{E}_{\omega \sim \mu} |\langle \check{f}(\omega), \psi(\omega, \mathbf{x}) \rangle|^2 &\leq \frac{C^2}{q} \mathbb{E}_{\omega \sim \mu} |\check{f}(\omega)|^2 \\ &= \frac{C^2 \|f\|_{\mathcal{H}_k}^2}{q}. \end{aligned}$$

An immediate consequence is the following corollary.

**Corollary 4** (Function Approximation). *For all  $\mathbf{x} \in \mathcal{X}$ ,  $\mathbb{E}_\omega |f(\mathbf{x}) - f_\omega(\mathbf{x})|^2 \leq \frac{C^2 \|f\|_{\mathcal{H}_k}^2}{q}$ .*

As a result, if  $\chi$  is a distribution on  $\mathcal{X}$ , we have

$$\begin{aligned} \mathbb{E}_\omega \|f - f_\omega\|_{2, \chi} &= \mathbb{E}_\omega \sqrt{\mathbb{E}_\chi |f(\mathbf{x}) - f_\omega(\mathbf{x})|^2} \\ &\leq \sqrt{\mathbb{E}_\omega \mathbb{E}_\chi |f(\mathbf{x}) - f_\omega(\mathbf{x})|^2} \\ &= \sqrt{\mathbb{E}_\chi \mathbb{E}_\omega |f(\mathbf{x}) - f_\omega(\mathbf{x})|^2} \\ &\leq \frac{C \|f\|_{\mathcal{H}_k}}{\sqrt{q}}. \end{aligned}$$

We next consider supervised learning with RFS. Let  $\mathcal{Y}$  be a target (output) space and let  $\ell : \mathbb{R}^t \times \mathcal{Y} \rightarrow \mathbb{R}_+$  be a  $\rho$ -Lipschitz loss function, i.e. for every  $y \in \mathcal{Y}$ ,  $|\ell(y_1, y) - \ell(y_2, y)| \leq \rho|y_1 - y_2|$ . Let  $\mathcal{D}$  be a distribution on  $\mathcal{X} \times \mathcal{Y}$ . We define the loss of a (prediction) function  $\mathbf{f} : \mathcal{X} \rightarrow \mathbb{R}^t$  as  $L_{\mathcal{D}}(\mathbf{f}) = \mathbb{E}_{(\mathbf{x}, y) \sim \mathcal{D}} \ell(\mathbf{f}(\mathbf{x}), y)$ . Let  $S = \{(\mathbf{x}_1, y_1), \dots, (\mathbf{x}_m, y_m)\}$  denote  $m$  i.i.d. examples sampled from  $\mathcal{D}$ . We denote by  $\mathcal{H}_k^t$  the space of all functions  $\mathbf{f} = (f_1, \dots, f_t) : \mathcal{X} \rightarrow \mathbb{R}^t$  where  $f_i \in \mathcal{H}_k$  for every  $i$ .  $\mathcal{H}_k^t$  is a Hilbert space with the inner product  $\langle \mathbf{f}, \mathbf{g} \rangle_{\mathcal{H}_k^t} = \sum_{i=1}^t \langle f_i, g_i \rangle_{\mathcal{H}_k}$ . Let  $\hat{\mathbf{f}}$  be the function in  $\mathcal{H}_k^t$  that minimizes the regularized empirical loss,

$$L_S^\lambda(\mathbf{f}) = \frac{1}{m} \sum_{i=1}^m \ell(\mathbf{f}(\mathbf{x}_i), y_i) + \lambda \|\mathbf{f}\|_{\mathcal{H}_k^t}^2,$$

over all functions in  $\mathcal{H}_k^t$ . It is well established (see e.g. Corollary 13.8 in [20]) that for every  $\mathbf{f}^* \in \mathcal{H}_k^t$ ,

$$\mathbb{E}_S L_{\mathcal{D}}(\hat{\mathbf{f}}) \leq L_{\mathcal{D}}(\mathbf{f}^*) + \lambda \|\mathbf{f}^*\|_{\mathcal{H}_k^t}^2 + \frac{2\rho^2}{\lambda m}. \quad (4)$$

If we further assume that  $\|\mathbf{f}^*\|_{\mathcal{H}_k^t} \leq B$ , for  $B > 0$ , and set  $\lambda = \frac{\sqrt{2}\rho}{\sqrt{m}B}$ , we obtain that

$$\mathbb{E}_S L_{\mathcal{D}}(\hat{\mathbf{f}}) \leq \inf_{\|\mathbf{f}^*\|_{\mathcal{H}_k^t} \leq B} L_{\mathcal{D}}(\mathbf{f}^*) + \frac{\sqrt{8}\rho B}{\sqrt{m}}. \quad (5)$$

The additive term in (5) is optimal, up to a constant factor. We would like to obtain similar bounds for an algorithm that minimizes the regularized loss w.r.t. the embedding  $\Psi_{\omega}$ . Let  $\hat{\mathbf{f}}_{\omega}$  be the function that minimizes,

$$L_S^{\lambda}(\mathbf{f}) = \frac{1}{m} \sum_{i=1}^m \ell(\mathbf{f}(\mathbf{x}_i), y_i) + \lambda \|\mathbf{f}\|_{\mathcal{H}_{k_{\omega}}^t}^2, \quad (6)$$

over all functions in  $\mathcal{H}_{k_{\omega}}^t$ . Note that in most settings  $\hat{\mathbf{f}}_{\omega}$  can be found efficiently by defining a matrix  $V \in \mathbb{C}^{t \times q}$  whose  $i$ 'th row is  $\mathbf{v}_i$ , and rewriting  $\hat{\mathbf{f}}_{\omega}$  as,

$$\hat{\mathbf{f}}_{\omega}(\mathbf{x}) = (\langle \mathbf{v}_1, \Psi_{\omega}(\mathbf{x}) \rangle, \dots, \langle \mathbf{v}_t, \Psi_{\omega}(\mathbf{x}) \rangle) \stackrel{\text{def}}{=} V \Psi_{\omega}(\mathbf{x}).$$

We now can recast the empirical risk minimization of (6) as,

$$L_S^{\lambda}(V) = \frac{1}{m} \sum_{i=1}^m \ell(V \Psi_{\omega}(\mathbf{x}_i), y_i) + \lambda \|V\|_{\text{F}}^2.$$

**Theorem 5** (Learning with RFS). *For every  $\mathbf{f}^* \in \mathcal{H}_k^t$ ,*

$$\mathbb{E}_{\omega} \mathbb{E}_S L_{\mathcal{D}}(\hat{\mathbf{f}}_{\omega}) \leq L_{\mathcal{D}}(\mathbf{f}^*) + \lambda \|\mathbf{f}^*\|_{\mathcal{H}_k^t}^2 + \frac{2\rho^2 C^2}{\lambda m} + \frac{\rho \|\mathbf{f}^*\|_{\mathcal{H}_k^t} C}{\sqrt{q}}. \quad (7)$$

*If we additionally impose the constraint  $\|\mathbf{f}^*\|_{\mathcal{H}_k^t} \leq B$  for  $B > 0$  and set  $\lambda = \frac{\sqrt{2}\rho C}{\sqrt{m}B}$  we have,*

$$\mathbb{E}_{\omega} \mathbb{E}_S L_{\mathcal{D}}(\hat{\mathbf{f}}_{\omega}) \leq \inf_{\|\mathbf{f}^*\|_{\mathcal{H}_k^t} \leq B} L_{\mathcal{D}}(\mathbf{f}^*) + \frac{\sqrt{8}\rho BC}{\sqrt{m}} + \frac{\rho BC}{\sqrt{q}}. \quad (8)$$

We note that for norm-efficient RFS (i.e. when  $C = 1$ ), if the number of random features is proportional to the number of examples, then the error terms in the bounds (8) and (5) are the same up to a multiplicative factor. Since the error term in (5) is optimal up to a constant factor, we get that the same holds true for (8).

*Proof.* For simplicity, we analyze the case  $t = 1$ . Since  $k_{\omega}$  is  $C$ -bonded, we have from (4) that,

$$\mathbb{E}_S L_{\mathcal{D}}(f) \leq L_{\mathcal{D}}(f^*) + \lambda \|f^*\|_{\mathcal{H}_{k_{\omega}}^t}^2 + \frac{2\rho^2 C^2}{\lambda m}.$$

Hence, it is enough to show that  $\mathbb{E}_\omega \|f_\omega^*\|_{\mathcal{H}_{k\omega}}^2 \leq \|f^*\|_{\mathcal{H}_k}^2$  and  $\mathbb{E}_\omega L_{\mathcal{D}}(f_\omega^*) \leq L_{\mathcal{D}}(f^*) + \frac{\rho \|f^*\|_{\mathcal{H}_k} C}{\sqrt{q}}$ . Indeed, since

$$f_\omega^*(\mathbf{x}) = \left\langle \frac{(\check{f}^*(\omega_1), \dots, \check{f}^*(\omega_q))}{\sqrt{q}}, \Psi_\omega(\mathbf{x}) \right\rangle,$$

we have, by Theorem 2,

$$\begin{aligned} \mathbb{E}_\omega \|f_\omega^*\|_{\mathcal{H}_{k\omega}}^2 &\leq \mathbb{E}_\omega \left[ \frac{\sum_{i=1}^q |\check{f}^*(\omega_i)|^2}{q} \right] \\ &= \frac{1}{q} \sum_{i=1}^q \mathbb{E}_{\omega_i} |\check{f}^*(\omega_i)|^2 \\ &= \|f^*\|_{\mathcal{H}_k}^2, \end{aligned}$$

and similarly,

$$\mathbb{E}_\omega L_{\mathcal{D}}(f_\omega^*) = \mathbb{E}_\omega \mathbb{E}_{\mathcal{D}} l(f_\omega^*(\mathbf{x}), y) = \mathbb{E}_{\mathcal{D}} \mathbb{E}_\omega l(f_\omega^*(\mathbf{x}), y).$$

Now, from the  $\rho$ -Lipschitzness of  $l$  and Theorem (4) we obtain,

$$\begin{aligned} \mathbb{E}_\omega l(f_\omega^*(\mathbf{x}), y) &\leq l(f^*(\mathbf{x}), y) + \rho \mathbb{E}_\omega |f^*(\mathbf{x}) - f_\omega^*(\mathbf{x})| \\ &\leq l(f^*(\mathbf{x}), y) + \rho \sqrt{\mathbb{E}_\omega |f^*(\mathbf{x}) - f_\omega^*(\mathbf{x})|^2} \\ &\leq l(f^*(\mathbf{x}), y) + \frac{\rho \|f^*\|_{\mathcal{H}_k} C}{\sqrt{q}}, \end{aligned}$$

concluding the proof.  $\square$

## 4 Random feature schemes for basic spaces

In order to apply Theorem 5, we need to control the boundedness of the generated features. Consider the RFS generation procedure, given in Algorithm 1, which employs multiplications of features generated from basic RFSs. If each basic RFS is  $C$ -bounded, then every feature that is a multiplication of  $t$  basic features is  $C^t$ -bounded. In light of this, we would like have RFSs for the basic spaces whose norm is as small as possible. The best we can hope for is *norm-efficient* RFSs—namely, RFSs with norm of 1. We first describe such RFSs for several kernels including the Gaussian kernel on  $\mathbb{R}^d$ , and the standard inner product on  $\mathbb{S}^0$  and  $\mathbb{S}^1$ . Then, we discuss the standard inner product on  $\mathbb{S}^{d-1}$  for  $d \geq 3$ . In this case, we show that the smallest possible norm for an RFS is  $\sqrt{d/2}$ . Hence, if the basic spaces are  $\mathbb{S}^{d-1}$  for  $d \geq 3$ , one might prefer to use other kernels such as the Gaussian kernel.

**Example 1** (Binary coordinates). Let  $\mathcal{X} = \{\pm 1\}$  and  $k(x, x') = xx'$ . In this case the deterministic identity RFS  $\psi(\omega, x) = x$  is norm-efficient.

**Example 2** (One dimensional sphere). Let  $\mathcal{X} = \mathbb{T}$  and  $k(z, z') = \langle z, z' \rangle$ . Let  $\psi(\omega, \mathbf{z}) = \mathbf{z}^\omega$ , where  $\omega$  is either  $-1$  or  $+1$  with equal probability. Then,  $\psi$  is a norm-efficient RFS since

$$\mathbb{E}_{\omega \sim \mu} \psi(\omega, z) \overline{\psi(\omega, z')} = \frac{zz' + \bar{z}\bar{z}'}{2} = \langle z, z' \rangle.$$

**Example 3** (Gaussian kernel). Let  $\mathcal{X} = \mathbb{R}^d$  and  $k(\mathbf{x}, \mathbf{x}') = e^{-\frac{a^2 \|\mathbf{x} - \mathbf{x}'\|^2}{2}}$ , where  $a > 0$  is a constant. The Gaussian RFS is  $\psi(\boldsymbol{\omega}, \mathbf{x}) = e^{ia\langle \boldsymbol{\omega}, \mathbf{x} \rangle}$ , where  $\boldsymbol{\omega} \in \mathbb{R}^d$  is the standard normal distribution. Then,  $\psi$  is a norm-efficient RFS, as implied by [16].

**Example 4** (Categorical coordinates). Let  $\mathcal{X} = [n]$  and define  $k(x, x') = 1$  if  $x = x'$  and 0 otherwise. In this case  $\psi(\omega, x) = e^{\frac{i\omega x}{2\pi n}}$ , where  $\omega$  is distributed uniformly over  $[n]$ , is a norm-efficient RFS since,

$$\mathbb{E}_{\omega \sim \mu} \psi(\omega, x) \overline{\psi(\omega, x')} = \mathbb{E}_{\omega} e^{\frac{i\omega(x-x')}{2\pi n}} = \begin{cases} 1 & x = x' \\ 0 & x \neq x' \end{cases}.$$

Examples 1 and 2 show that the standard inner product on the sphere in one and two dimensions admits a norm-efficient RFS. We next examine the sphere  $\mathbb{S}^{d-1}$  for  $d \geq 3$ . In this case, we show a construction of a  $\sqrt{d}/2$ -bounded RFS. Furthermore, we show that it is the best attainable bound. Namely, any RFS for  $\mathbb{S}^{d-1}$  will necessarily have a norm of at least  $\sqrt{d}/2$ . In particular, there does not exist a norm-efficient RFS when  $d \geq 3$ .

**Example 5** ( $\mathbb{S}^{d-1}$  for  $d \geq 3$ ). Let  $\mu$  be the uniform distribution on  $\Omega = [d] \times \{-1, +1\}$ . Define  $\psi : \Omega \times \mathbb{S}^{d-1} \rightarrow \mathbb{C}$  for  $\omega = (j, b)$  as  $\psi(\omega, \mathbf{x}) = \sqrt{d}/2(x_j + ibx_{j+1})$ , where we use the convention  $x_{d+1} := x_1$ . Now,  $\psi$  is a  $\sqrt{d}/2$ -bounded RFS as,

$$\begin{aligned} & \mathbb{E}_{(j,b) \sim \mu} \psi((j, b), \mathbf{x}) \overline{\psi((j, b), \mathbf{x}')} \\ &= \frac{d}{2} \frac{\sum_{j=1}^d [(x_j + ix_{j+1})(x'_j - ix'_{j+1}) + (x_j - ix_{j+1})(x'_j + ix'_{j+1})]}{2d} \\ &= \frac{\sum_{j=1}^d [x_j x'_j + x_{j+1} x'_{j+1}]}{2} \\ &= \langle \mathbf{x}, \mathbf{x}' \rangle. \end{aligned}$$

We find it instructive to compare the RFS above to the following  $\sqrt{d}$ -bounded RFSs.

**Example 6.** Let  $\mu$  be the uniform distribution on  $\Omega = \mathbb{S}^{d-1}$  and define  $\psi : \Omega \times \mathbb{S}^{d-1} \rightarrow \mathbb{R}$  as  $\psi(\mathbf{w}, \mathbf{x}) = \sqrt{d} \langle \mathbf{w}, \mathbf{x} \rangle$ . We get that,

$$\mathbb{E}_{\mathbf{w} \sim \mu} [\psi(\mathbf{w}, \mathbf{x}) \psi(\mathbf{w}, \mathbf{x}')] = d \mathbb{E}_{\mathbf{w} \sim \mu} \langle \mathbf{w}, \mathbf{x} \rangle \langle \mathbf{w}, \mathbf{x}' \rangle = d \langle \mathbf{x}, W \mathbf{x}' \rangle,$$

where  $W_{i,j} = \mathbb{E}_{\mathbf{w} \sim \mu} [w_i w_j]$ . Since  $\mathbf{w}$  is distributed uniformly on  $\mathbb{S}^{d-1}$ ,  $\mathbb{E} [w_i w_j] = 0$  for  $i \neq j$  and  $\mathbb{E} [w_i^2] = 1/d$ . Thus, we have  $W = (1/d)\mathbb{I}$  and therefore  $\mathbb{E}_{\mathbf{w} \sim \mu} [\psi(\mathbf{w}, \mathbf{x}) \psi(\mathbf{w}, \mathbf{x}')] = \langle \mathbf{x}, \mathbf{x}' \rangle$ . A similar result still holds when  $\psi(\omega, \mathbf{x}) = \sqrt{d} x_\omega$  where  $\omega \in [d]$  is distributed uniformly.

To conclude the section, we prove that  $\sqrt{d}/2$ -boundedness is optimal for RFS on  $\mathbb{S}^{d-1}$ .

**Theorem 6.** *Let  $d \geq 1$  and  $\epsilon > 0$ . There does not exist a  $(\sqrt{d}/2 - \epsilon)$ -bounded RFS for the kernel  $k(\mathbf{x}, \mathbf{x}') = \langle \mathbf{x}, \mathbf{x}' \rangle$  on  $\mathbb{S}^{d-1}$ .*

Before proving the theorem, we need the following lemmas.

**Lemma 7.** Let  $\mathbf{z} \in \mathbb{C}^d$ . There exists  $\mathbf{a} \in \mathbb{S}^{d-1}$  such that  $\left| \sum_j a_j z_j \right|^2 \geq \frac{1}{2} \|\mathbf{z}\|^2$ .

*Proof.* Let us write  $\mathbf{z} = \boldsymbol{\alpha} + i\boldsymbol{\beta}$  where  $\boldsymbol{\alpha}, \boldsymbol{\beta} \in \mathbb{R}^d$ . We thus have  $\|\mathbf{z}\|^2 = \|\boldsymbol{\alpha}\|^2 + \|\boldsymbol{\beta}\|^2$ . We can further assume that  $\|\boldsymbol{\alpha}\|^2 \geq \frac{1}{2} \|\mathbf{z}\|^2$  as otherwise we can replace  $\mathbf{z}$  with  $i\mathbf{z}$ . Let us define  $\mathbf{a}$  as  $\boldsymbol{\alpha}/\|\boldsymbol{\alpha}\|$ . We now obtain that,

$$\left| \sum_j a_j z_j \right|^2 \geq \langle \mathbf{a}, \boldsymbol{\alpha} \rangle^2 = \|\boldsymbol{\alpha}\|^2 \geq \frac{1}{2} \|\mathbf{z}\|^2,$$

which concludes the proof.  $\square$

**Lemma 8.** Let  $(\psi, \mu)$  be an RFS for the kernel  $k(\mathbf{x}, \mathbf{x}') = \langle \mathbf{x}, \mathbf{x}' \rangle$  on  $\mathbb{S}^{d-1}$  and let  $\mathbf{a} \in \mathbb{S}^{d-1}$ . Then, for almost all  $\omega$  we have  $\psi(\omega, \mathbf{a}) = \sum_{j=1}^d a_j \psi(\omega, \mathbf{e}_j)$ .

*Proof.* Let us examine the difference between  $\Psi^{\mathbf{a}} \stackrel{\text{def}}{=} \psi(\cdot, \mathbf{a})$  and  $\sum_j a_j \Psi^{\mathbf{e}_j} \stackrel{\text{def}}{=} \sum_j a_j \psi(\cdot, \mathbf{e}_j)$ ,

$$\begin{aligned} & \left\| \Psi^{\mathbf{a}} - \sum_{i=1}^d a_i \Psi^{\mathbf{e}_i} \right\|_{L^2(\Omega)}^2 \\ &= \langle \Psi^{\mathbf{a}}, \Psi^{\mathbf{a}} \rangle_{L^2} + \sum_{i,j=1}^d a_i a_j \langle \Psi^{\mathbf{e}_i}, \Psi^{\mathbf{e}_j} \rangle_{L^2} - 2 \sum_{i=1}^d a_i \langle \Psi^{\mathbf{a}}, \Psi^{\mathbf{e}_i} \rangle_{L^2} \\ &= \langle \mathbf{a}, \mathbf{a} \rangle + \sum_{i,j=1}^d a_i a_j \langle \mathbf{e}_i, \mathbf{e}_j \rangle - 2 \sum_{i=1}^d a_i \langle \mathbf{a}, \mathbf{e}_i \rangle \\ &= \left\| \mathbf{a} - \sum_{i=1}^d a_i \mathbf{e}_i \right\|^2 = 0. \end{aligned}$$

$\square$

*Proof of Theorem 6.* Let  $\psi : \mathbb{S}^{d-1} \times \Omega \rightarrow \mathbb{C}$  be an RFS for  $k(\mathbf{x}, \mathbf{x}') = \langle \mathbf{x}, \mathbf{x}' \rangle$  and let  $\epsilon > 0$ . We next show that  $\psi$  is not  $\sqrt{d/2} - \epsilon$ -bounded. Let  $A \subset \mathbb{S}^{d-1}$  be a dense and countable set. From Lemma (8) and the fact that sets of measure zero are closed under countable union, it follows that for almost every  $\omega$  and all  $\mathbf{a} \in A$  we have  $\psi(\omega, \mathbf{a}) = \sum_{i=1}^d a_i \psi(\omega, \mathbf{e}_i)$ . Using the linearity of expectation we know that,

$$\mathbb{E}_{\omega \sim \mu} \sum_{i=1}^d |\psi(\omega, \mathbf{e}_i)|^2 = \sum_{i=1}^d \mathbb{E}_{\omega \sim \mu} |\psi(\omega, \mathbf{e}_i)|^2 = \sum_{i=1}^d \langle \mathbf{e}_i, \mathbf{e}_i \rangle = d.$$

Hence, with a non-zero probability we get,

$$\sum_{i=1}^d |\psi(\omega, \mathbf{e}_i)|^2 > d - \epsilon, \tag{9}$$

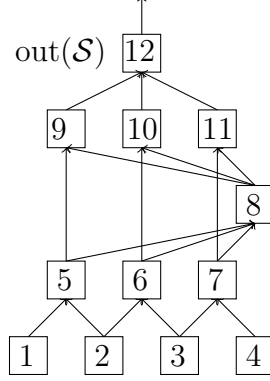


Figure 1: An illustration of a computation skeleton.

and,

$$\forall \mathbf{a} \in A, \psi(\omega, \mathbf{a}) = \sum_{i=1}^d a_i \psi(\omega, \mathbf{e}_i). \quad (10)$$

Let us now fix  $\omega$  for which (9) holds. From Lemma (7) there exists  $\tilde{\mathbf{a}} \in \mathbb{S}^{d-1}$  such that  $|\sum_i \tilde{a}_i \psi(\omega, \mathbf{e}_i)|^2 \geq \frac{d-\epsilon}{2}$ . Since  $A$  is dense in  $\mathbb{S}^{d-1}$  there is a vector  $\mathbf{a} \in A$  for which  $|\sum_i a_i \psi(\omega, \mathbf{e}_i)|^2 \geq \frac{d}{2} - \epsilon$ . Finally, from (9) it follows that  $|\psi(\omega, \mathbf{a})|^2 \geq \frac{d}{2} - \epsilon$ .  $\square$

## 5 Compositional random feature schemes

Compositional kernels are obtained by sequentially multiplying and averaging kernels. Hence, it will be useful to have RFSs for multiplications and averages of kernels. The proofs of Lemmas 9 and 10 below are direct consequences of properties of kernel spaces and RFSs and thus omitted.

**Lemma 9.** *Let  $(\psi^1, \mu^1), (\psi^2, \mu^2), \dots$  be RFSs for the kernels  $k^1, k^2, \dots$  and let  $(\alpha_i)_{i=1}^\infty$  be a sequence of non-negative numbers that sum to one. Then, the following procedure defines an RFS for the kernel  $k(\mathbf{x}, \mathbf{x}') = \sum_{i=1}^n \alpha_i k^i(\mathbf{x}, \mathbf{x}')$ .*

1. Sample  $i$  with probability  $\alpha_i$
2. Choose  $\omega \sim \mu^i$
3. Generate the feature  $\mathbf{x} \mapsto \psi_\omega^i(\mathbf{x})$

**Lemma 10.** *Let  $(\psi^1, \mu^1), \dots, (\psi^n, \mu^n)$  be RFSs for the kernels  $k^1, \dots, k^n$ . The following scheme is an RFS for the kernel  $k(\mathbf{x}, \mathbf{x}') = \prod_{i=1}^n k^i(\mathbf{x}, \mathbf{x}')$ . Sample  $\omega_1, \dots, \omega_n \sim \mu^1 \times \dots \times \mu^n$  and generate the feature  $\mathbf{x} \mapsto \prod_{i=1}^n \psi_{\omega_i}^i(\mathbf{x})$ .*

**Random feature schemes from computation skeletons.** We next describe and analyze the case where the compositional kernel is defined recursively using a concrete computation graph defined below. Let  $\mathcal{X}_1, \dots, \mathcal{X}_n$  be measurable spaces with corresponding normalized kernels  $k^1, \dots, k^n$  and RFSs  $\psi^1, \dots, \psi^n$ . We refer to these spaces, kernels, and RFS as *base spaces*, kernels and RFSs. We also denote  $\mathcal{X} = \mathcal{X}_1 \times \dots \times \mathcal{X}_n$ . The base spaces (and correspondingly kernels, and RFSs) often adhere to a simple form. For example, for real-valued input, feature  $i$  is represented as  $\mathcal{X}_i = \mathbb{T}$ , where  $k^i(z, z') = \langle z, z' \rangle$ ,  $\psi_\omega^i(z) = z^\omega$ , and  $\omega$  is distributed uniformly in  $\{\pm 1\}$ .

We next discuss the procedure for generating compositional RFSs using a structure termed *computation skeleton*, or *skeleton* for short. A skeleton  $\mathcal{S}$  is a DAG with  $m := |\mathcal{S}|$  nodes.  $\mathcal{S}$  has a single node whose out degree is zero, termed the *output node* and denoted  $\text{out}(\mathcal{S})$ , see Figure 1 for an illustration. The nodes indexed 1 through  $n$  are input nodes, each of which is associated with a base space. We refer to non-input nodes as internal nodes. Thus, the indices of internal nodes are in  $\{n + 1, \dots, m\}$ . An internal node  $v$  is associated with a PSD function (called a conjugate activation function [6][Sec. 5]),  $\hat{\sigma}_v(\rho) = \sum_{i=0}^{\infty} a_i^v \rho^i$ . For every node  $v$  we denote by  $\mathcal{S}_v$  the subgraph of  $\mathcal{S}$  rooted at  $v$ . This sub-graph defines a compositional kernel through all the nodes nodes with a directed path to  $v$ . By definition it holds that  $\text{out}(\mathcal{S}_v) = v$  and  $\mathcal{S}_{\text{out}(\mathcal{S})} = \mathcal{S}$ . We denote by  $\text{in}(v)$  the set of nodes with a directed edge into  $v$ . Each skeleton defines a kernel  $k_{\mathcal{S}} : \mathcal{X} \times \mathcal{X} \rightarrow \mathbb{R}$  according to the following recurrence,

$$k_{\mathcal{S}}(\mathbf{x}, \mathbf{x}') = \begin{cases} k_v(\mathbf{x}, \mathbf{x}') & v \in [n] \\ \hat{\sigma}_v\left(\frac{\sum_{u \in \text{in}(v)} k_{\mathcal{S}_u}(\mathbf{x}, \mathbf{x}')}{|\text{in}(v)|}\right) & v \notin [n] \end{cases} \quad \text{for } v = \text{out}(\mathcal{S}).$$

In Figure 1 we give the pseudocode describing the RFS for the kernel  $k_{\mathcal{S}}$ . We call the routine **RFSS** as a shorthand for a Random Feature Scheme for a Skeleton. The correctness of the algorithm is a direct consequence of Lemmas 9 and 10.

---

**Algorithm 1** RFSS( $\mathcal{S}$ )

---

```

Let  $v = \text{out}(\mathcal{S})$ 
if  $v \in [n]$  then
  Return  $\mathbf{x} \mapsto \psi^v(\mathbf{x})$ 
else
  Sample  $l \in \{0, 1, 2, \dots\}$  according to  $(a_i^v)_{i=0}^{\infty}$ 
  for  $j = 1, \dots, l$  do
    Choose  $u \in \text{in}(v)$  at random
    Call RFSS( $\mathcal{S}_u$ ) and get  $\mathbf{x} \mapsto \psi_{\omega_j}(\mathbf{x})$ 
  end for
  Return  $\mathbf{x} \mapsto \prod_{j=1}^l \psi_{\omega_j}(\mathbf{x})$ 
end if

```

---

We next present a simple running time analysis of Algorithm 1 and the sparsity of the generated random features. Note that a compositional random feature is a multiplication of base random features. Thus the amortized time it takes to generate a compositional random

feature and its sparsity amount to the expected number of recursive calls made by RFSS. For a given node  $v$  the expected number of recursive calls emanating from  $v$  is,

$$\mathbb{E}_{l \sim (a_j^v)} [l] = \sum_{j=0}^{\infty} j a_j = \hat{\sigma}'(1).$$

We now define the *complexity* of a skeleton as,

$$\mathcal{C}(\mathcal{S}) = \begin{cases} 1 & \text{out}(\mathcal{S}) \in [n] \\ \hat{\sigma}'_v(1) \frac{\sum_{u \in \text{in}(v)} \mathcal{C}(\mathcal{S}(u))}{|\text{in}(v)|} & \text{otherwise} \end{cases}. \quad (11)$$

It is immediate to verify that  $\mathcal{C}(\mathcal{S})$  is the expected value of the number of recursive calls and the sparsity of a random feature. When all conjugate activations are the same (11) implies that

$$\mathcal{C}(\mathcal{S}) \leq (\hat{\sigma}'(1))^{\text{depth}(\mathcal{S})},$$

where equality holds when the skeleton is layered. For activations such as ReLU,  $\sigma(x) = \max(0, x)$ , and exponential,  $\sigma(x) = e^x$ , we have  $\hat{\sigma}'(1) = 1$ , and thus  $\mathcal{C}(\mathcal{S}) = 1$ . Hence, it takes constant time in expectation to generate a random feature, which in turn has a constant number of multiplications of base random features. For example, let us assume that the basic spaces are  $\mathbb{S}^1$  with the standard inner product, and that the skeleton has a single non-input node, equipped with the exponential dual activation  $\hat{\sigma}(\rho) = e^\rho$ . In this case, the resulting kernel is the Gaussian kernel and  $\mathcal{C}(\mathcal{S}) = 1$ . Therefore, the computational cost of storing and evaluating each feature is constant. This is in contrast to the Rahimi and Recht scheme [16], in which the cost is linear in  $n$ .

## 6 Empirical Evaluation

**Accuracy of kernel approximation.** We empirically evaluated the kernel approximation of our random feature scheme under kernels of varying structure and depth. Our concern is efficiency of random features: how does the quality of approximation fare in response to increasing the target dimension of the feature map? Theorem 3 already establishes an upper bound for the approximation error (in high probability), but overlooks a few practical advantages of our construction that are illustrated in the experiments that follow. Primarily, when one repeatedly executes Algorithm 1 in order to generate features, duplicates may arise. It is straightforward to merge them and hence afford to generate more under the target feature budget. We use the CIFAR-10 dataset for visual object recognition [11].

We considered two kernel structures, one *shallow* and another *deep*. Figure 2 caricatures both. For visual clarity, it oversimplifies convolutions and the original image to one-dimensional objects, considers only five input pixels, and disregards the true size and stride of convolutions used.

Following Daniely et al. [6], for a scalar function  $\sigma : \mathbb{R} \rightarrow \mathbb{R}$  termed an activation, let  $\hat{\sigma}(\rho) = \mathbb{E}_{(X,Y) \sim N_\rho} [\sigma(X)\sigma(Y)]$  be its conjugate activation (shown in the original to be a PSD function). Our shallow structure is simply a Gaussian (RBF) kernel with scale 0.5.

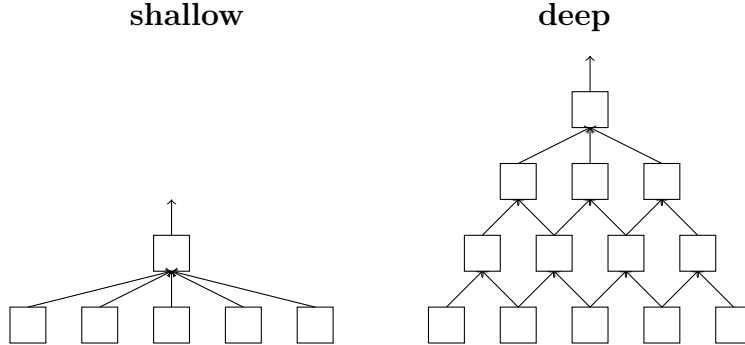


Figure 2: Simple illustration of the skeleton structures corresponding to the shallow (left) and deep (right) settings in evaluating the approximation (Figure 3). The deep setting considers two layers of convolutions followed by one that is fully connected.

Equivalently, again borrowing the terminology of Daniely et al. [6], it corresponds to a single-layer fully-connected skeleton, having a single internal node  $v$  to which all input nodes point. The node  $v$  is labeled with a conjugate activation  $\hat{\sigma}_v(\rho) = \exp((\rho - 1)/4)$ .

The deep structure comprises a layer of 5x5 convolutions at stride 2 with a conjugate activation of  $\hat{\sigma}_1(\rho) = \exp((\rho - 1)/4)$ , followed by a layer of 4x4 convolutions at stride 2 with the conjugate activation  $\hat{\sigma}_2$  corresponding to the ReLU activation  $\sigma_2(t) = \max\{0, t\}$ , followed by a fully-connected layer again with the ReLU’s conjugate activation.

In each setting, we compare to a natural baseline built (in part, where possible) on the scheme of Rahimi and Recht [16] for Gaussian kernels. In the shallow setting, doing so is straightforward, as their scheme applies directly. As their scheme is not defined for compositional kernels, our baseline in the deep setting is a hybrid construction. A single random features is generated according to the recursive procedure of Algorithm 1, until an internal node is reached *in the bottom-most convolutional layer*. Each such node corresponds to a Gaussian kernel, and so we apply the scheme Rahimi and Recht [16] to approximate the kernel of that node.

For each configuration of true compositional kernel and feature budget, we repeat the following ten times: draw a batch of 128 data points at random (each center-cropped to 24x24 image pixels), generate a randomized feature map, and compute  $128^2$  kernel evaluations. The result is  $10 \cdot 128^2$  corresponding evaluations of the true kernel  $k$  and an empirical kernel  $\hat{k}$ . We compare error measures and correlation between the two kernels using (i) RFS inner products as the empirical kernel and (ii) inner products from the baseline feature map. Figure 3 plots the comparison.

**Structural effects and relation to neural networks.** In connection to deep neural networks, we experiment with the effect of compositional kernel architecture on learning. We explore two questions: (i) Is a convolutional structure effective in a classifier built on random features? (ii) What is the relation between learning a compositional kernel and a neural network corresponding to its skeleton? The second question is motivated by the connection that Daniely et al. [6] establish between a compositional kernel and neural networks

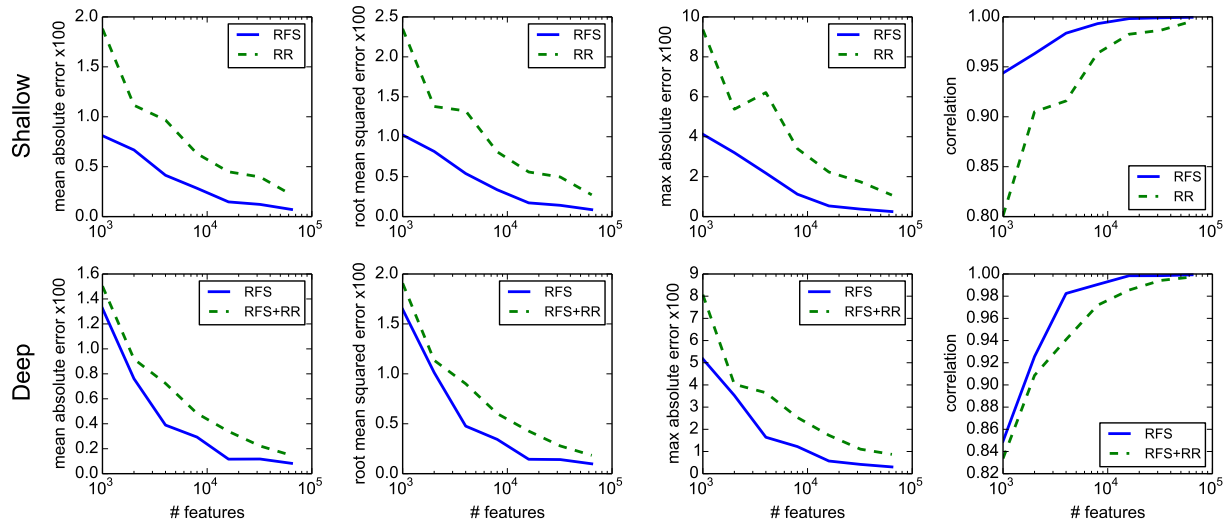


Figure 3: Comparisons of the mean-absolute, root-mean-squared, and maximum differences, as well as the correlation, between an empirical kernel and the ground truth kernel. RFS denotes our construction. In the shallow setting, the baseline (RR) is the scheme of Rahimi and Recht [16] for Gaussian kernels. In the deep setting, the baseline (RFS+RR) uses the recursive sampling scheme of RFS to arrive at a first-level convolution, and then mimics RR on the convolution patch. The RFS approximation is dominant in every comparison.

Arch	RFS	Net	Gap	Rank
4,5	72.88	77.09	4.21	1
6,4	72.42	77.06	4.64	2
6,6	72.25	75.52	3.27	4 (-1)
4,4	71.49	74.94	3.45	6 (-2)
5,4	71.45	76.78	5.33	3 (+2)
4,6	70.62	74.24	3.62	7 (-1)
5,6	70.39	75.38	4.99	5 (+2)
6,5	70.14	74.23	4.09	8
5,5	69.64	73.57	3.93	9
Full	60.01	55.09	-4.92	10

Table 1: Comparison of test accuracy of kernel learning with RFS and neural networks. For each architecture test we provide its ranking in terms of performance and relative rank ordering. The column designated as “Arch” describes the convolution size as pairs  $a,b$  where the first layer convolution is of size  $axa$  and the second is  $bxb$ .

described by its skeleton. In particular, we first explore the difference in classification accuracy between the kernel and the network. Then, since training under the kernel is simply a convex problem, we ask whether its relative accuracy across architectures predicts well the relative performance of analogous fully-trained networks.

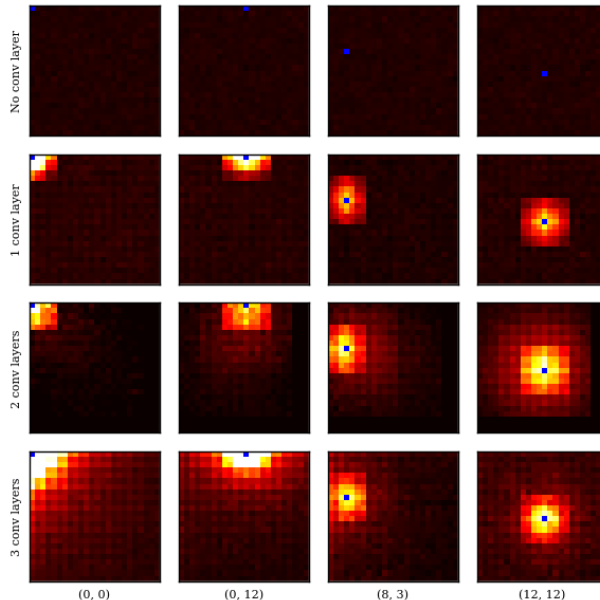


Figure 4: Illustration of the local structure captured by the our random feature scheme. We generated 500,000 random features corresponding to four kernels - a flat kernel with one fully connected hidden layer, and three deep kernels with one, two and three convolution layers with ReLU activations. The figures above show the correlations of 4 pixels (in blue) with all other pixels; lighter colors denote higher correlation.

For the experiment, we considered several structures and trained both a corresponding networks and the compositional kernel through an RFS approximation. We again use the CIFAR-10 dataset, with a standard data augmentation pipeline [12]: random 24x24 pixel crop, random horizontal flip, random brightness, saturation, and contrast delta, per-image whitening, and per-patch PCA. In the test set, no data augmentation is applied, and images are center-cropped to 24x24. We generated  $10^6$  random features, and trained for 120 epochs with AdaGrad [7] and a manually tuned initial learning rate among  $\{25, 50, 100, 200\}$ .

The convolutional architectures are of the same kind as the deep variety in Sec. 6, i.e. two convolutions with a size between 4x4 and 6x6 and a stride of 2, followed by a fully-connected layer. The fully-connected architecture is the shallow structure described in Section 6. All activations are ReLU. The per-patch PCA preprocessing step projects patches to the top  $q$  principal components where  $q$  is 10, 12, and 16, respectively, for first-layer convolutions of size 4, 5, and 6, respectively. The neural networks are generated from the kernel’s skeleton by node replication (i.e. producing channels) at a rate of 64 neurons per skeleton node for convolutions and 384 for fully-connected layers. We use the typical random Gaussian initialization [8], 200 epochs of AdaGrad with a manually tuned initial learning rate among  $\{.0002, .0005, .001, .002, .005\}$ .

Test set accuracies are given in Table 1, annotated with how well approximate RFS learning accuracies rank those of the trained networks. We would like to underscore that, for convolutional kernels, networks consistently outperformed the kernel. Meanwhile, the fully-connected kernel actually outperforms the corresponding network. RFS learning moreover

ranks the top two networks correctly (as well as the bottom three). This observation is qualitatively in line with earlier findings of Saxe et al. [17], who final-layer training of a randomly initialized network to rank fully-trained networks. Indeed, from Daniely et al. [6], we know that the random network approach is an alternative random feature map for the compositional kernel.

**Visualization of hierarchical random features.** In Figure 4, we illustrate how our random feature scheme is able to accommodate local structures that are fundamental to image data. We chose 4 different networks of varying depths, and generated 500,000 random features for each. We then computed for each pixel, the probability that it co-occurs in a random feature with any other pixel, by measuring the correlation between their occurrences. As expected, for the flat kernel, the correlation between any pair of pixels was the same. However for deeper kernels, nearby pixels co-occur more often in the random features, and the degree of this co-occurrence is shown in the figure. As we increase the depth, different tiers of locality appear. The most intense correlations share a common first-layer convolution, while moderate correlation share only a second-layer convolution. Lastly, mild correlation share no convolutions.

## References

- [1] F. Bach. Breaking the curse of dimensionality with convex neural networks. *arXiv:1412.8690*, 2014.
- [2] F. R. Bach. On the equivalence between quadrature rules and random features. *CoRR*, abs/1502.06800, 2015. URL <http://arxiv.org/abs/1502.06800>.
- [3] L. Bo, K. Lai, X. Ren, and D. Fox. Object recognition with hierarchical kernel descriptors. In *Computer Vision and Pattern Recognition (CVPR), 2011 IEEE Conference on*, pages 1729–1736. IEEE, 2011.
- [4] Y. Cho and L.K. Saul. Kernel methods for deep learning. In *Advances in neural information processing systems*, pages 342–350, 2009.
- [5] Amit Daniely. Sgd learns the conjugate kernel class of the network. *arXiv:1702.08503*, 2017.
- [6] Amit Daniely, Roy Frostig, and Yoram Singer. Toward deeper understanding of neural networks: The power of initialization and a dual view on expressivity. In *Advances In Neural Information Processing Systems*, pages 2253–2261, 2016.
- [7] John Duchi, Elad Hazan, and Yoram Singer. Adaptive subgradient methods for online learning and stochastic optimization. *Journal of Machine Learning Research*, 12(Jul): 2121–2159, 2011.
- [8] X. Glorot and Y. Bengio. Understanding the difficulty of training deep feedforward neural networks. In *International conference on artificial intelligence and statistics*, pages 249–256, 2010.

- [9] K. Grauman and T. Darrell. The pyramid match kernel: Discriminative classification with sets of image features. In *Tenth IEEE International Conference on Computer Vision*, volume 2, pages 1458–1465, 2005.
- [10] P. Kar and H. Karnick. Random feature maps for dot product kernels. *arXiv:1201.6530*, 2012.
- [11] A. Krizhevsky, I. Sutskever, and G. Hinton. Learning multiple layers of features from tiny images. Technical report, University of Toronto, 2009.
- [12] A. Krizhevsky, I. Sutskever, and G.E. Hinton. Imagenet classification with deep convolutional neural networks. In *Advances in neural information processing systems*, pages 1097–1105, 2012.
- [13] J. Mairal. End-to-End Kernel Learning with Supervised Convolutional Kernel Networks. In *Advances in Neural Information Processing Systems (NIPS)*, 2016.
- [14] J. Mairal, P. Koniusz, Z. Harchaoui, and Cordelia Schmid. Convolutional kernel networks. In *Advances in Neural Information Processing Systems*, pages 2627–2635, 2014.
- [15] J. Pennington, F. Yu, and S. Kumar. Spherical random features for polynomial kernels. In *Advances in Neural Information Processing Systems*, pages 1837–1845, 2015.
- [16] A. Rahimi and B. Recht. Random features for large-scale kernel machines. In *NIPS*, pages 1177–1184, 2007.
- [17] A. Saxe, P.W. Koh, Z. Chen, M. Bhand, B. Suresh, and A.Y. Ng. On random weights and unsupervised feature learning. In *Proceedings of the 28th International Conference on Machine Learning (ICML-11)*, pages 1089–1096, 2011.
- [18] B. Schölkopf, C. Burges, and A. Smola, editors. *Advances in Kernel Methods - Support Vector Learning*. MIT Press, 1998.
- [19] B. Schölkopf, P. Simard, A. Smola, and V. Vapnik. Prior knowledge in support vector kernels. In *Advances in Neural Information Processing Systems 10*, pages 640–646. MIT Press, 1998.
- [20] S. Shalev-Shwartz and S. Ben-David. *Understanding Machine Learning: From Theory to Algorithms*. Cambridge University Press, 2014.
- [21] V. N. Vapnik. *Statistical Learning Theory*. Wiley, 1998.
- [22] V.N. Vapnik. *The Nature of Statistical Learning Theory*. Springer, 1995.